



Available online at www.sciencedirect.com

ScienceDirect

Procedia Manufacturing 13 (2017) 13–20

Procedia
MANUFACTURING

www.elsevier.com/locate/procedia

Manufacturing Engineering Society International Conference 2017, MESIC 2017, 28-30 June 2017, Vigo (Pontevedra), Spain

Cutting-tool wear characterization by means of conoscopic holography

P. Zapico, D. Blanco*, C. Cuervo, G. Valiño, J.C. Rico

IPF Research Group, Dept. of Construction and Manufacturing Engineering, University of Oviedo, Campus of Gijón, Gijón 33203, Spain

Abstract

The ability of Conoscopic Holography (CH) to provide accurate digitizing of tool wear is analysed in this work. Firstly, tests have been conducted to check out the performance of the sensor when digitizing inserts without chip breaker geometry, which have been artificially worn using electro-discharge machining (EDM). A methodology for determining the number of digitizing orientations has been also developed, in order to achieve best results in surface reconstruction. Secondly, digitizing tests have been carried upon inserts with chip breaker geometry and different grades of wear. Results support the use of CH.

© 2017 The Authors. Published by Elsevier B.V.

Peer-review under responsibility of the scientific committee of the Manufacturing Engineering Society International Conference 2017.

Keywords: Conoscopic Holography, Tool Wear, Digitizing

1. Introduction

Tool wear is among the key aspects that influence the quality of machined parts in many ways: it conditions the relative positioning between tool and part, which affects dimensional accuracy; it modifies chip flow over the rake surface of the tool; it also conditions the structural integrity of the tool. Therefore, characterization of cutting tool wear turns out to be an important issue, which is the reason why it has been the subject of numerous studies over the past decades.

* Corresponding author. Tel.: +34 985 18 2444

E-mail address: dbf@uniovi.es

On-line characterization of tool wear seems to be the best option from an operational point of view, since real time monitoring of tool condition results in a greater control over the process. Nevertheless, the techniques that are commonly used for on-line monitoring (like forces, vibrations or acoustic emission) are greatly affected by the particularities of each application. Moreover, they cannot really provide a direct control of tool wear magnitude, since they are all indirect methods. In fact, cutting conditions, tool geometry or even signal processing methods severely affect in-cycle techniques capacity to characterize the wear. At this moment, there is no reliable and universal approach to the problem of on-line monitoring of tool wear [1].

On the other hand, although in-cycle characterization techniques have certain advantages, they force the interruption of machining operation in order to allow direct observation of tool surfaces. Nevertheless, they can provide a more reliable and universal wear characterization, frequently through the calculation of the classic wear parameters (flank wear width or VB and depth of the crater or KT). This capacity has motivated the work of an important number of researchers, who employ very different techniques to characterize the wear. These techniques can be classified into two categories depending on the use of bi-dimensional or three-dimensional approach.

Most in-cycle tool wear monitoring applications have addressed the inherent difficulties of discrimination between both the worn out area and the intact one. The integration of artificial vision equipment, either in the machine itself or in attached installations, does not present a special difficulty. However, good lighting of the tool is often pointed out as a key issue for subsequent image processing [2]. Hence, Zhang [3] incorporates an additional source of LED lighting to improve the quality and sharpness of digital tool images. There are also other factors that complicate the task of delineating the precisely worn zone. As a consequence, there are several examples of different methods used to determine a boundary between the worn and the intact area, like the evaluation of grey level difference [3] or statistical descriptors [4]. Nevertheless, it seems clear that these techniques suffer when transforming two-dimensional information into a geometric boundary, and they also present problems for the correct interpretation of anomalies as the built-up edge.

3D reconstruction techniques of cutting tool geometry could be a more robust option, since they use to be less dependent on ambient lighting and they permit simultaneous digitizing of different tool surfaces without requiring multiple orientations. Finally, although accurate identification of the boundary between wear and intact surface is still an issue, it is possible to model the intact surfaces and then calculate worn surface deviations. Different technologies can be used for 3D digitizing of tool surfaces. These include white light interferometry [5,6], which provides good results regardless of the geometric characteristics. However, this technique has two disadvantages: it is an expensive technology and it cannot be easily integrated in a production machine. This prevents the use of white light interferometry for in-cycle on-machine monitoring. Another option is the use of the phase shifting method [7]. In this work, fringe patterns with various phase-shifts are projected onto the rake face of the tool, upon which four grey-level images are captured. 3D information is then reconstructed and KT is calculated. This method is useful because the images are taken at one time, but it has the problem that the orientation of both the Charged Coupled Device (CCD) and the projector must be configured in each case for each tool.

Laser projection techniques offer some advantages. Čerče et al. [8,9] used a Keyence 2D laser profile sensor combined with a displacement stage for in-cycle evaluation of tool wear in a lathe. They obtained 3D representation of tool condition evolution through a particular machining operation. The evolution of the comparison between each 3D point cloud and the original not-wear tool allows not only to identify crater wear, but also to find small amounts of material adhered to the tool (Built Up Edge). They extracted bi-dimensional profiles in order to evaluate classical wear indicators, such as VB and KT, and to represent the evolution of flank and crater wear. Nevertheless, like all triangulation systems, laser triangulation is conditioned by accessibility issues (like occlusion effects), related to the angle between laser projection and CCD orientation.

It can be noticed that all those techniques have advantages and disadvantages. However, Conoscopic Holography (CH) is a three-dimensional digitizing technique that has some robust features. CH is a coherent light interferometry technique based on the double refractive property of uniaxial crystals. It was developed by Sirat and Psaltis in 1984 [10]. In 1999 it was improved and patented by Sirat as Linear Conoscopic Holography [11]. Linear HC has been shown to have good accuracy properties in a wide variety of materials. Since HC is collinear technique (the direction of projection of the laser and the direction of observation are identical), it is capable of digitizing surfaces with great slope, avoiding occlusion effects while maintaining acceptable accuracy. In addition, the use of different lenses allows to easily adapt the measuring range and tune the sensor according to each task requirements.

Present work aims on the evaluation of Linear CH ability to record and characterize the wear of cutting tools. This objective has been addressed in two different tasks: on the first one, the ability of CH for characterizing artificially-induced wear upon inserts without chip breaker geometry is analysed; on the second one, digitizing tests are carried out upon inserts with chip breaker geometry and different grades of wear.

2. Materials and methods

A linear CH sensor ConoPoint 10, integrated in a CMM DEA Swift A001, has been used for digitizing tasks. This machine is also equipped with a contact measurement sensor. In terms of performance, it has been certified with Maximum Permissible Probing Tolerance (MPE_P) and Maximum Permissible Linear Measuring Tolerance (MPE_E) as shown in Table 1. The CH sensor is connected to the encoders of the machine, so that the instantaneous reading of the distance to the object is synchronized in real time with the positions of the axes. There are several issues regarding the configuration of the sensor, which comprise aspects relative to both the hardware and the software. Hence, the selection of a proper lens conditions the working range and the metrological performance of the equipment. Two lenses have been considered in this work: a 25 mm focal length lens and a 50 mm one. Several data regarding the performance of these lenses are shown in Table 1.

Table 1. CMM and lenses properties.

Characteristic	L25	L50	CMM property	Value (μm)
DOF	mm	1.8	8	4
Standoff	mm	14	44	$4+4 \cdot 10^{-3} \cdot L$
Repeatability	μm	0.06	0.10	<i>*Being L in mm</i>
X laser spot size	μm	27	37	
Angular coverage	$^\circ$	150	170	

Laser power (P) and capture frequency (F) are the most important configuration parameters of this type of sensors. P is a dimensionless parameter that take values in the range from 0 to 4095 (equivalent to a 0 - 100% range). Maximum absolute power is under 1mW (Class 2, IEC 60825-1: 2007). On the other hand, the F parameter sets the sensor measurement capture frequency, allowing values in the range from 50 to 9000 Hz.

These parameters should be configured taking into account the optical properties of the surface and its orientation with respect to projection of the laser beam, the type and characteristics of selected lens or the environmental conditions. To achieve optimum setup, the sensor associates two quality parameters with each capture: SNR (Signal-to-Noise Ratio) and Total. The SNR represents the quality of the detected signal, while the Total reflects the amount of light received by the sensor during capture. Good quality digitizing demands a minimum 50% SNR and a Total value between 1200 and 21000, according to the recommendations of the manufacturer.

In this particular integration, the sensor was mounted on the carriage of the machine, with the laser beam is pointing vertically and downwards. Therefore, it is possible to perform scans by moving the X and Y axes of the machine while recording, for each XY location, the distance between surface and sensor. In addition, the encoders of the axes of the machine were connected to the sensor by means of the OPS (Optimet Position Synchronizer) communication Box. This allows to assign a position of axes to each capture realized by the sensor. Two calibrations are needed: the intrinsic calibration of the sensor is provided by the manufacturer, whereas the extrinsic one, relating sensor data to the reference system of the machine, has been performed using a method developed in a previous work [12]. Two different inserts have been used in this work (Fig. 1).



Fig. 1. (a) Sandvik Coromant CCMW 09 T3 04 5015; (b) ISCAR TGMF 635-080.

3. HC digitizing of simulated artificial tool wear

The ability to detect artificially-generated wear on a standard insert has been evaluated using a Sandvik Coromant CCMW 09 T3 04 5015 insert (Fig. 1a) without chip-breaker geometry. This tool has 83° cutting edge angle. Additionally, a 25 mm lens has been employed in the HC sensor. Work started by determining optimum orientations between the projection of the laser beam and the relevant areas of insert: zones adjacent to cutting edge in both rake and flank surfaces. The objective of this effort is to establish whether a single orientation could provide quality digitizing of those surfaces, or else several orientations (typically one orientation for each surface) are needed. In order to achieve this objective, the ideal situation should be maximizing signal quality (regarding SNR) and accuracy for both rake and flank surfaces.

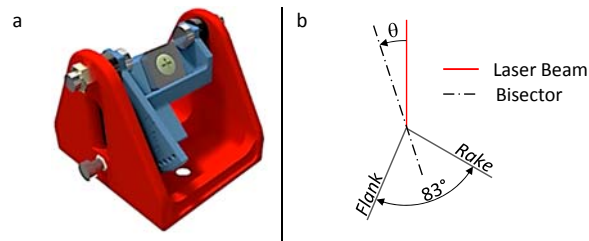


Fig. 2. (a) Fixture; (b) Angular reference scheme.

Therefore, the insert should be digitized according to different insert orientations to perform quality comparisons. Nevertheless, this purpose meets an early problem concerning the ideal set-up values for configuration parameters P and F, since different optima would be obtained depending on the angle of incidence of the laser beam. Therefore, preliminary tests were performed with different laser incidence angles. As a result of this analysis, F has been set to a 1500Hz value, and P has been set to a 67%.

This particular insert has flat rake and flank surfaces. Such circumstance simplifies this analysis, since the evolution of quality results for a particular surface is symmetrical with respect to the bisector of the edge angle. To determine the optimal orientation angle, an ad hoc fixture was employed (Fig. 2a). This fixture allows the insert to be tilted in a range $\theta = \pm 53.5^\circ$ with respect to an orientation where the laser beam is parallel to the bisector of the edge angle (Fig. 2b). This fixture also permits indexed positioning with a first step of 3.5° and ten steps of 5° , for each direction.

Sixty points located on rake surface have been obtained for every tested laser orientation. Then, an average value for the SNR has been calculated, so that the overall quality of the cloud, according to signal quality, can be compared: the higher SNR, the better signal quality. Additionally, surface flatness is calculated for every orientation and its resultant value is compared with a reference one. In this tests, a reference value of 0.004 mm has been obtained from touch-probe digitizing using the same CMM. Therefore, a so-called “flatness error” is calculated as the difference between flatness value (for each orientation) and the reference one. This indicator has been used to evaluate the quality of surfaces digital reconstruction.

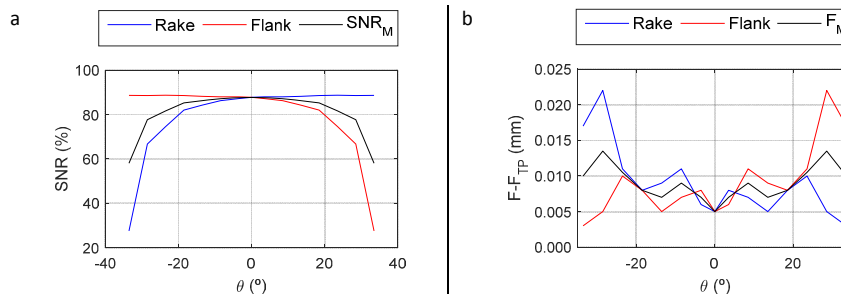


Fig. 3. Results of the test: (a) SNR; Flatness Error (b).

The graphs in Fig. 3 contain values for SNR (a) and flatness error (b) from rake surface in a blue colour. Moreover, since it has been established that quality behaviour is symmetric, expected values corresponding to flank surface are represented in a red colour. Finally, black lines are used to provide mean value for the two indicators, considering both surfaces simultaneously. It can be observed that average both signal and geometric reconstruction qualities get worse when tilting the fixture from the neutral orientation.

Having a closer look at each surface behaviour, it can be observed that SNR experiments a slight improvement when tilting takes laser beam orientation closer to each surface normal, whereas the opposite effect (SNR drops heavily) is taken place simultaneously for the other surface. The overall effect, considering both surfaces simultaneously through the mean value, causes a maximum for the 0° orientation. Taken flatness in consideration, relatively similar behaviour could be observed. Although calculated error varies abruptly with incidence angle, the overall trend is to get worse when the beam increases its tilt with respect to the normal to each surface. Nevertheless, the neutral (0°) orientation provokes a mean flatness error of 0.005 mm simultaneously in both surfaces. Both results allow to conclude that using a single neutral orientation provides acceptable values according to both the SNR and the flatness criteria, in rake and flank surfaces simultaneously. The consequence is that the areas of interest on the insert could be digitized using a fixed fixture (Fig. 4).



Fig. 4. Insert located on the fixed fixture.

A regular wear was provoked into the reference insert using a flat EDM (electro-discharge machining) electrode. A portion of the volume from the edge zone was removed according to the scheme shown in Fig. 5. This causes the boundary between worn and intact zones to be a straight line, parallel to the initial edge. This procedure was repeated twice, so 0.60 mm and 0.98 mm VB flank wear have been successively obtained (h parameter). The insert was digitized before and after each EDM operation, so the resultant point clouds could be later compared. Digitized area was limited to a 7×2.5 mm extension, and the sample resolution was 0.050×0.004 mm.

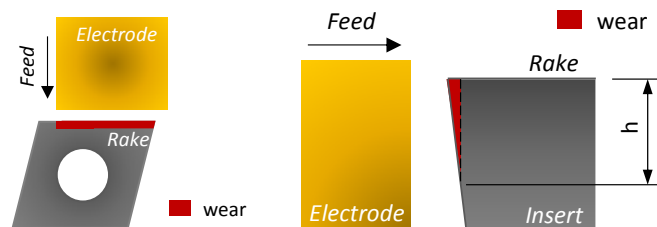


Fig. 5. Schematic representation of EDM electrode and insert.

Fig. 6 shows a comparison between the three phases of wearing: intact (the blue one), the 0.6 mm VB (the yellow one) and the 0.98 mm VB (the red one). The HC sensor shows its capacity for an accurate characterization of tool wear, using one single orientation. Additionally, using this 3D technique, new parameters could be calculated and they could help to improve wear characterization. One example is the value of worn volume. This parameter can be obtained in a CAD environment, since it is possible to build a solid that matches the volume comprised between the intact insert surface and the worn one. Once this solid has been built, its volume can be easily determined by the CAD software itself.

Table 2. Worn volumes.

H (mm)	W_V^T (mm ³)	W_V (mm ³)
0.60	0.090	0.082
0.98	0.247	0.250

Table 2 provides values for worn volume (W_V) calculated for each wear grade following this procedure and the corresponding theoretical ones (W_V^T), which were calculated assuming the EDM programmed depth to be true. As can be noticed, the differences between the measured worn volumes values and the theoretical ones are very small (under 10%). These differences could be partially related to geometry simplifications (i.e. the tool radius) of the theoretical CAD model, whereas there is also a slight contribution of the uncertainty of the measuring method. Nevertheless, this circumstance does not hugely affect the final result.

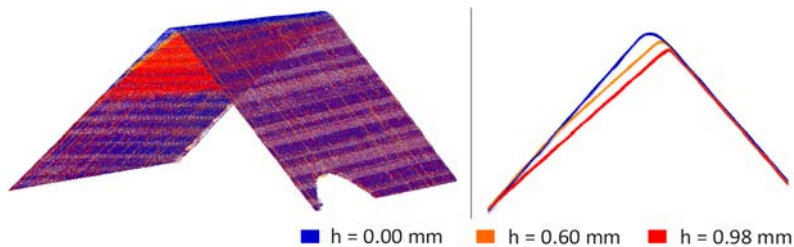


Fig. 6. A comparison between intact and worn surfaces for the standard insert (two levels).

4. HC digitizing of actual tool wear

In the second part of this work, the ability of HC for characterizing actual tool wear has been evaluated using an ISCAR TGMF 635-080 insert. This tool has a complex rake surface chip-breaker geometry. This implies that, even if the orientation of the laser beam is fixed, its actual incidence angle will take different values along the rake surface. So that, even it is not possible to establish a single optimal orientation for the rake surface. Therefore, it is not possible for both rake and flank surfaces.

To overcome this problem, a series of digitizing tests have been carried out to select a proper orientation in order to get a proper quality in both rake and flank surfaces. Focus have been pointed at getting a good representation of flank surface and an acceptable one of rake surface: loss of points due to low quality takes place mainly in positions located far from the edge of the tool, in areas that have no real interest for wear measurement. In this part of the work, a 50 mm lens was used because of its greater angular coverage (Table 1).

Setup parameters were configured so that the whole area of interest could be digitized under SNR and Total acceptable values. Previous tests had led to a configuration with 600Hz F and 100% P. The inserts were selected between a series of units that had been previously used in CNC machining of sintered metal parts. Two inserts (two specimens per insert), covering different kinds of tool wear, were employed in this work. Digitized surface was restricted to a 7 x 10 mm area, according the XY coordinates, and assuring a correct coverage of the edge of the tool and adjacent areas. Resolution was 0.065 mm (X) and 0.020 mm (Y). An ad-hoc fixed fixture was designed and manufactured in PLA (polylactide) using fused filament fabrication.

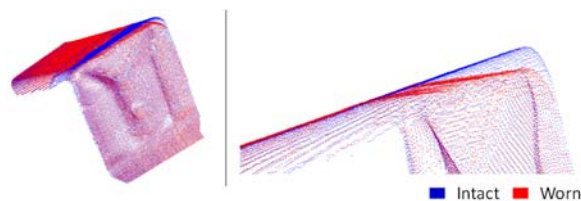


Fig. 7. A comparison between intact and worn surfaces for the ISCAR inserts.

In this case, the intact geometry was not available, since inserts were only digitized after being worn. Nevertheless, an intact insert was also digitized, and the resulting point cloud has been used as “intact geometry” for comparison purposes. This condition has demanded an alignment procedure using common non-wear zones in intact insert and worn inserts. The reverse engineering Geomagic Studio software has been used for this task. Fig. 7 shows a comparison between two point clouds: one corresponding to the intact insert (blue cloud) and one of the worn inserts (red cloud). Wear zone can easily be identified as both clouds match one another almost completely, with the only exception of a worn volume in the proximities of the original edge.

The inserts were observed using a Nikon SMZ2T stereomicroscope in order to compare its images with 3D digitized point cloud. An ad hoc indicator has been used for comparison (W_{Lmax}). It represents the maximum length of the worn zone, as measured in the orthogonal direction to the edge: as is to say, the maximum distance between the edge and the boundary of the worn zone. This indicator, alongside with wear volume, (calculated following the same procedure that has been described in the first part of this work) are presented in Table 3. Two columns are given for W_{Lmax} , since this parameter was obtained from both the microscopy images (W_{Lmax}^M) and the 3D point clouds (W_{Lmax}).

Table 3. Values adopted by wear indicators.

Specimen	W_V (mm ³)	W_{Lmax} (mm)	W_{Lmax}^M (mm)
1	0.020	0.33	0.37
2	0.140	1.05	1.06
3	0.560	1.24	1.29
4	0.020	0.27	0.31

Finally, Fig. 8 provides three representations of each single insert: microscopic view of the flank surface (left), 3D representation of the whole insert (centre) and isolated wear volumes (right). It can be observed the capacity of HC to capture wear volumes that can be distinguished in a yellow colour in the central images.

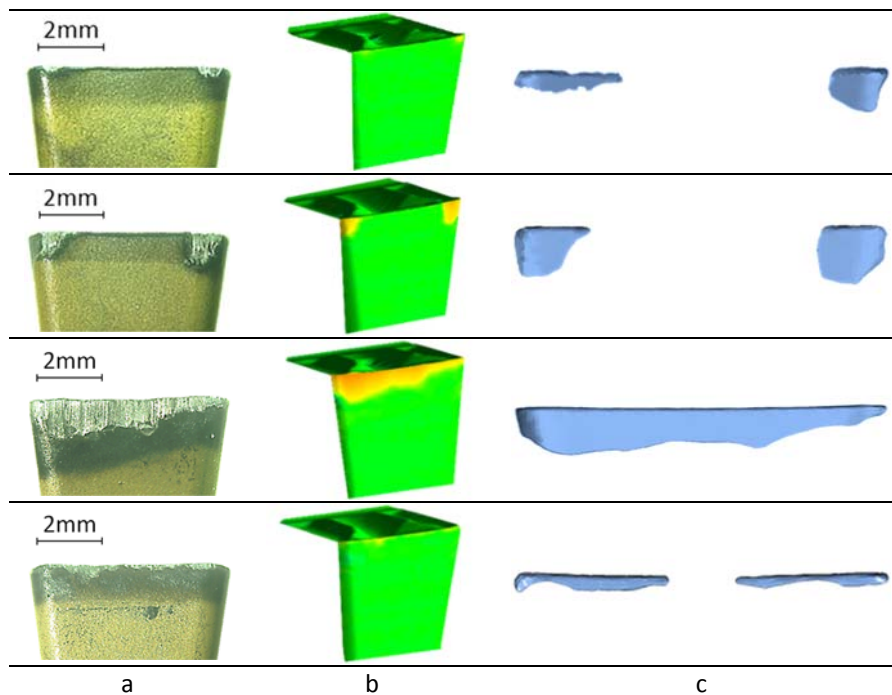


Fig. 8. Representation of tool wear: (a) Microscopy images; (b) 3D comparison between intact and worn inserts, (c) isolated worn volume.

5. Conclusions

In present work, the capability of linear conoscopic holography for tool wear monitoring has been analysed. Digitizing tests have been carried out using a conventional insert with an artificially worn edge to check out CH robustness and reliability. Tests have probed that the sensor is capable of digitizing both rake and flank surfaces using one single orientation, whereas providing an accurate representation of 3D wear. An estimation of worn zone dimensions has been extracted from 3D point clouds, and the results match fairly well the theoretical values. Moreover, an estimation of worn volume can also be calculated from this virtually reconstructed model. In the second part of this work, test were carried upon tool inserts that had been worn during actual industrial machining operations. Comparison between 3D data from the CH sensor and 2D images obtained using microscopy probe that conoscopy could provide fairly accurate data, that could be used in many ways: calculation on 2D classic wear parameters (such as VB or KT) or a more complex extraction of newly-defined parameters (like worn volume).

Due to its robustness, it seems possible to integrate a CH sensor in a CNC machine, without compromising this machine's behaviour. Results show that CH us a promising technique that could serve, in the future, as the basis of an in-cycle tool-condition monitoring solution.

Further work should be carried out to provide a complete demonstration of this technique, maybe by using a CH sensor in a progressive wear test under controlled conditions in a laboratory environment. Such a test would set the fundamentals for an integral industrial-degree solution.

Acknowledgements

This work was supported by the Regional Ministry of Economy and Employment of the Principality of Asturias (Spain) (GRUPIN14-063) and the Government of the Principality of Asturias through the Programme "Severo Ochoa" 2014 of PhD grants for research and teaching (BP14-049).

References

- [1] A. Siddhpura, R. Paurobally, *Int. J. Adv. Manuf. Technol.* 65 (2013) 371–393.
- [2] S. Dutta, S.K. Pal, S. Mukhopadhyay, R. Sen, *CIRP J. Manuf. Sci. Technol.* 6 (2013) 212–232.
- [3] C. Zhang, J. Zhang, *Comput. Ind.* 64 (2013) 708–719.
- [4] E. Alegre, R. Aláiz, J. Barreiro, M. Viñuela. *Lect. Notes Comput. Sci.* 3773 (2005).
- [5] A. Devillez, S. Lesko, W. Mozer, *Wear.* 256 (2004) 56–65.
- [6] A. Zawada-Tomkiewicz, B. Storch, *Pomiary Autom. Kontrola.* 56 (2010) 950–953.
- [7] W.H. Wang, Y.S. Wong, G.S. Hong, *Wear* 261 (2006) 164–171.
- [8] L. Čerče, F. Pušavec, J.Kopač, *J. Mech. Eng.* 61(2015) 489–497.
- [9] L. Čerče, F. Pušavec, J.Kopač, *J. Mech. Sci. Technol.* 29 (2015) 3885–3895.
- [10] G. Sirat, D. Psaltis, *Opt. Lett.* 10 (1985) 4–6.
- [11] G. Sirat. *Linear Conoscopic Holography*, US Patent 5953137 (1999).
- [12] P. Fernández, D. Blanco, G. Valiño, V. Hoang, L. Suárez y S. Mateos, *Integration of a conoscopic holography sensor on a CMM. Proceedings of 4th Manufacturing Society International Conference (MESIC 2011). Cádiz, Spain, 2011.*